8. Supplementary material

8.1. Computing added mass inertia

The standard method for computing mean added mass is to treat the added mass as a cylindrical volume of fluid that surrounds the wing [13]. The dimensions of the cylinder are defined by the dimensions of the wing: the radius is half the mean chord length, $\bar{c}/2$, the length is single wing span R measured from wing hinge to wing tip, and the density is the fluid density ρ. The added rotational inertia is thus the rotational inertia of a cylinder of mass m_A that rotates about its base:

$$m_A = \rho\frac{\pi}{4}R\bar{c}^2$$
$$I_A = \frac{1}{16}m_A\bar{c}^2 + \frac{1}{3}m_AR^2$$

In our system, with $\bar{c} = 3.5$ cm, $R = 10$ cm, $\rho_{H_2O} = 977\ \frac{kg}{m^3}$, added mass inerita $I_A = 3.465 \times 10^{-4}\ kg\ m^2$.

8.2. Structural damping modeling

Structural damping for generic oscillatory motion can be represented as an additional complex term in the spring stiffness parameter:

$$K = k(1 + i\gamma) \tag{32}$$

However, this representation is not convenient for numerical modeling because of the complex term. If we assume that the oscillatory motion is sinusoidal, it is possible to express structural damping another way. Beginning with a generic spring-wing equation

$$I_t\ddot{x} + k(1 + i\gamma)x + \Gamma\dot{x}^2 = 0$$

we make the substitutions $x = Xe^{i\omega t}$ and $\dot{x} = i\omega Xe^{i\omega t}$:

$$I_t\ddot{x} + kXe^{i\omega t} + \gamma kiXe^{i\omega t} + \Gamma\dot{x}^2 = 0$$

Using the definition $\frac{\dot{x}}{\omega} = iXe^{i\omega t}$, we can rearrange:

$$I_t\ddot{x} + kx + \frac{\gamma k}{\omega}\dot{x} + \Gamma\dot{x}^2 = 0 \tag{33}$$

Thus, the structural damping term can be represented as a viscous damper that is normalized by the oscillation frequency, implying frequency-independent viscous damping.

8.3. Derivation of the non-dimensional spring-wing equations

We introduce dimensionless time and angle parameters normalized to wing oscillation amplitude and frequency:

$$\tau = \omega t,\ q_w = \frac{\theta}{\theta_0},\ \dot{q}_w = \frac{\dot{\theta}}{\omega\theta_0},\ \ddot{q}_w = \frac{\ddot{\theta}}{\omega^2\theta_0}$$

Plugging these terms into Eq. 7 and rearranging coefficients, we obtain

$$I_t\theta_0\omega^2\ddot{q}_w + k_p\theta_0 q_w + \frac{\gamma k_p}{\omega}\omega\theta_0 q_w + \Gamma\theta_0^2\omega^2|\dot{q}_w|\dot{q}_w = T(t)$$

$$\ddot{q}_w + \frac{k_p}{I_t\omega^2}q_w + \frac{\gamma k_p}{I_t\omega^2}\dot{q}_w + \frac{\Gamma\theta_0}{I_t}|\dot{q}_w|\dot{q}_w = \frac{T(t)}{I_t\theta_0\omega^2}$$

$$\ddot{q}_w + \hat{K}_p q_w + \gamma\hat{K}_p\dot{q}_w + \frac{1}{N}|\dot{q}_w|\dot{q}_w = \hat{T}_p(t) \tag{34}$$

Eq. 34 is a forced nonlinear oscillator defined by non-dimensional parameters $\hat{K}$, the reduced stiffness; γ, the structural damping loss modulus; and N, the Weis-Fogh number.

Performing a similar substitution for the series system we arrive at the equation

$$\ddot{q}_w + \hat{K}_s q_w + \gamma\hat{K}_s\dot{q}_w + \frac{1}{N}|\dot{q}_w|\dot{q}_w = \hat{T}_s(t) \tag{35}$$

which is identical to Eq. 34 except for the normalized torque, which is now defined as

$$\hat{T}_s(t) = \frac{\hat{K}_s}{\theta_0}\left(\phi(t) + \frac{\gamma}{\omega}\dot{\phi}\right) \tag{36}$$

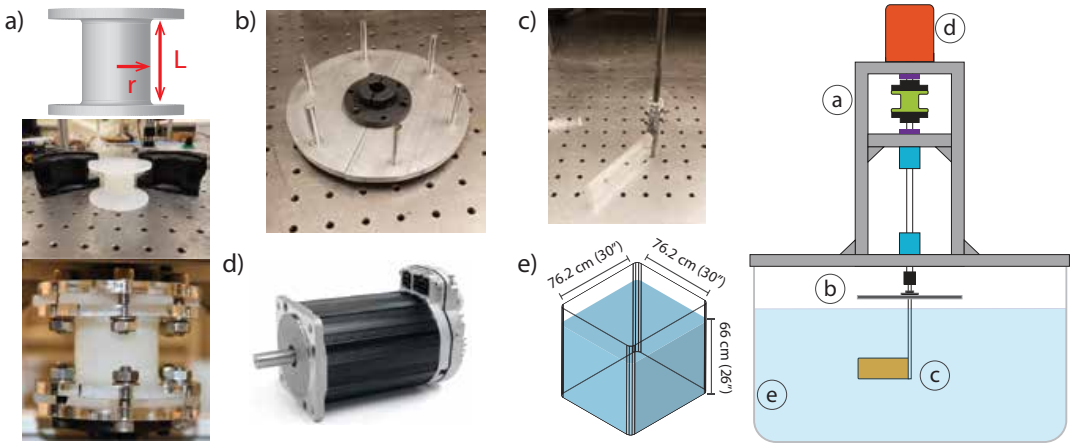

Figure 12. Robophysical system component detail. A diagram of the system is shown at the right, with labels for each of the components. a) the design process of the silicone torsion spring, from 3D CAD model based on desired dimensions to 3D-printed mold for silicone to completed spring with acrylic adapter plates and steel flange couplers. b) An aluminum inertia plate used to change the overall system inertia. c) The fixed-pitch acrylic wing with aluminum hub and 1/4" steel shaft. d) Teknic Clearpath SDSK Motor used to drive the system (photo from Teknic). e) Dimensions of the 115-gallon rectangular tank (Chem-Tainer) as well as water depth.

8.4. Robophysical system details

In Figure 12 we show the elements of the robophysical system. The left column of Fig. 12 shows the design process of the silicone torsion spring, from 3D CAD model based on desired dimensions (top-left) to 3D-printed mold for silicone (mid-left) to completed spring with acrylic adapter plates and steel flange couplers (bottom-left). In Fig. 12b we show the aluminum inertia plate that was used to change the overall system inertia. Fig. 12c shows the fixed-pitch acrylic wing with aluminum hub and 1/4" steel shaft. We used a Teknic Clearpath SDSK Motor used to drive the system (12d). The dimensions of the 115-gallon rectangular tank as well as water depth are shown in Fig. 12e.

8.5. Computing drag torque coefficient

We follow the standard methods for blade-element analysis of quasi-steady flapping wings. The wing is broken into differential chord elements, each of which experiences a differential aerodynamic torque,

$$\mathrm{d}Q_{aero} = \frac{1}{2} r\rho \left(r\dot{\theta}\right)^2 C_D(\alpha) c(r) \mathrm{d}r \tag{37}$$

The differential torques along the wing can be integrated across the entire wing shape resulting in the following equations

For simplicity we express the velocity dependence of the aerodynamic torque as, $\dot{\theta}^2$, and the sign dependence on the direction of motion is implied. The aerodynamic torque is governed by both the wing speed and the aerodynamic torque constant, Γ,

which itself is a function of wing geometry (wing radial length, R and shape factor r_3), wing pitch angle (α), and fluid density (ρ). The drag coefficient, $C_D(\alpha)$, is dependent on the pitch angle of the wing, α, which is 0 when the wing is vertical, and $\pi/2$ when the wing is horizontal. From Dickinson [10] the drag coefficient at insect-relevant Reynolds numbers is estimated as

$$C_D(\alpha) = 1.92 - 1.55\cos(2.04\alpha - 9.82) \tag{38}$$

8.6. Design and fabrication of silicone springs

We designed and 3D-printed two-piece molds for casting the springs. Each mold was treated with Ease Release 200^{TM} (Smooth On) before being filled with a common silicone material used in soft-robotics, Dragonskin^{TM} 30A silicone (Smooth-On) [29]. Care was taken to de-gas the silicone in a vacuum chamber before filling the mold. The silicone molds were allowed to cure in a positive pressure chamber for at least 24 hours before removal and use.

The dimensions of the springs were determined by the desired spring stiffness. The torsional stiffness of a silicone spring is given by the stiffness equation for a twisting cylinder:

$$k_s = \frac{\mu\pi R^4}{2L} \tag{39}$$

where μ is the shear modulus, R is the spring radius, and L is the spring length. We used three spring designs of constant length and radius 13, 16, 18 mm corresponding to torsional stiffness values of k_s = [0.163, 0.416,0.632] Nm/rad.

8.7. Data Processing

Analysis of both experiment and simulation data relied on the wing and motor angle data. To generate a consistent sampling time of all experiments we interpolated position measurements to a constant sample rate. The measured angle data was filtered with a 5th-order Butterworth filter at cutoff frequency of 10Hz (approximately 2.5 times greater than the peak driving frequency). Velocity was computed through numerical differentiation of the filtered position, and similarly acceleration from the filtered velocity.

We observed that the wing trajectories were consistent with a single frequency sin wave except when actuation frequency or amplitude approached the epxerimental limits (at low-amplitude and high-frequency and at high-amplitude). We used a nonlinear least-squares sine fit to find amplitude and phase of the motor, $\phi(t)$, and wing, $\theta(t)$, trajectories respectively.

8.8. Derivation of non-dimensional resonance frequency for series system

The following derivation is based on the process in [6]. For a system with a spring with stiffness k in series with an actuator that drives a mass m subject to aerodynamic loading, $\Gamma\dot{x}^2$, the power driving the mass, P_w is the sum of the aerodynamic and inertial forces times the velocity:

$$P_m = (F_a + F_i)\dot{x} = (\Gamma\dot{x}^2 + m\ddot{x})\dot{x} \tag{40}$$

The strain energy in the spring, E, is

$$E = \frac{1}{2}k^{-1}(F_a + F_i) = \frac{1}{2}k^{-1}\left(\Gamma\dot{x}^2 + m\ddot{x}\right)^2 \tag{41}$$

Since the motor must both move the mass and compress the spring, the actuator power, P_{act}, is defined

$$\begin{aligned} P_{act} &= P_m + \dot{E} \\ P_{act} &= \left(\Gamma\dot{x}^2 + m\ddot{x}\right)\left[\dot{x} + k^{-1}\left(2\Gamma\dot{x}\ddot{x} + m\dddot{x}\right)\right] \end{aligned} \tag{42}$$

If we assume that the mass follows a sinusoidal trajectory, $x(t) = x_0 \sin\omega t$, we can compute the derivatives and plug into 42:

$$P_{act} = x_0^2\omega^3 \cos\omega t\left[\Gamma x_0 \cos^2\omega t - m\sin\omega t\right]\left[1 - k^{-1}\omega^2(2\Gamma x_0 \sin\omega t + m)\right] \tag{43}$$

If we define a non-dimensional actuator power, $\hat{P}_{act} = \frac{P_{act}}{mx_0^2\omega^3}$, we can get the non-dimensional expression:

$$\hat{P}_{act} = \cos\omega t\left(N^{-1}\cos^2\omega t - \sin\omega t\right)\left[1 - \hat{K}^{-1}(2N^{-1}\sin\omega t + 1)\right] \tag{44}$$

Bennett et al. showed that this actuator power expression is minimized over half an oscillation period when it is always greater than zero. The relationship between $\hat{K}$ and N that guarantees that condition is

$$\hat{K} = \sqrt{1 + 4N^{-2}} \tag{45}$$

Eq. 45 describes the of spring, mass, aerodynamic damping and oscillation amplitude to get resonant oscillation at a particular frequency. Recalling that $\hat{K} = \frac{k}{m\omega^2}$, $N = \frac{m}{\Gamma x_0}$, and natural frequency $\omega_n^2 = \frac{k}{m}$ we can get an expression for that frequency:

$$\omega_r^2 = \frac{k}{\sqrt{m^2 + 4\Gamma^2 x_0^2}} = \frac{\omega_n^2}{\sqrt{1 + 4N^{-2}}} \tag{46}$$

8.9. Derivation of non-dimensional wing torques in the parallel system

Here we provide the full derivation for the non-dimensional work presented in Eq. 28 and 29. We start from the non-dimensional force terms in the parallel system dynamics (Eqn. 8). We make the assumption of sinusoidal wing motion, such that

$$\begin{aligned} q &= \sin(\tau) \\ \dot{q} &= \cos(\tau) \\ \ddot{q} &= -\sin(\tau) \\ &= -q \end{aligned}$$

Substituting these expressions in for the individual force terms in the parallel system and multiplying by the aerodynamic force in those equations results in

$$\begin{aligned} \tilde{Q}_{aero} &= \cos^2(\tau) \\ \tilde{Q}_{inertial} &= -Nq \\ \tilde{Q}_{idealelastic} &= \hat{K}Nq \\ \tilde{Q}_{structural} &= \gamma\hat{K}N\cos(\tau) \end{aligned}$$

In order to write $\tilde{Q}_{aero}$ and $\tilde{Q}_{structural}$ in terms of wing angle we can use the following trigonometric relationship

$$\begin{aligned} \cos^2(\tau) &= 1 - \sin^2(\tau) \\ &= 1 - q^2 \qquad (47) \\ \cos(\tau) &= \sqrt{1-q^2} \qquad (48) \end{aligned}$$

Substituting in the expressions of $\cos(\tau)$ and $\cos^2(\tau)$ yields the non-dimensional work equations in terms of just the normalized wing angle, q.

8.10. Derivation of non-dimensional wing torque due to viscous damping

We can use the same method as in the above section to show that the relationship between the Weis-Fogh number N and the dynamic efficiency holds true even if we change the damping model. If we choose a viscous damping model where torque is proportional to velocity, $\tau_{viscous} = c_v\dot{\theta}$, we can get the non-dimensional torque term as in Eq. 8:

$$\hat{\tau}_{viscous} = \frac{c_v\theta_o\omega}{I\theta_o\omega^2}\dot{q} = 2\zeta\sqrt{\hat{K}}\dot{q} \qquad (49)$$

where we have used the standard definition of the harmonic-oscillator damping ratio, $\zeta = \frac{c_v}{2I\omega_n}$. The damping ratio must be less than one for resonance to be possible.

Multiplying by the maximum aerodynamic force, we arruve at the non-dimensional torque

$$\tilde{Q}_{viscous} = 2\zeta N\sqrt{\hat{K}}\cos(\tau) = 2\zeta N\sqrt{\hat{K}(1-q^2)} \tag{50}$$

which scales linearly with N, the same as the structural damping torque. Therefore, viscous damping leads to a dynamic efficiency that monotonically decreases with the Weis-Fogh number resulting in the same qualitative result as with structural damping.